JOURNAL OF SOLID STATE CHEMISTRY 13, 182–191 (1975)

Phase Relations, Dopant Effects, Structure, and High Electrical Conductivity in the Na_2WO_4–Na_2MoO_4 System

P. H. BOTTELBERGHS AND F. R. VAN BUREN

Department of Inorganic Chemistry, Croesestraat 77A, Utrecht, The Netherlands

Received April 25, 1974

The x, T-phase diagram of the binary system Na_2WO_4–Na_2MoO_4 has been redetermined at ambient pressure, taking into account the influence of hysteresis effects. Thermodynamic calculations, based upon transition entropies as determined by precision DSC (differential scanning calorimetry), indicate that the system is almost ideal with respect to the high-temperature phases.

As anion dopes, Na_2SO_4 and Na_2CrO_4 give a metastable extension of the β-phase of Na_2WO_4 at decreasing temperature, involving some 40°C at 0.01 mole fraction of dopant. Cation dopes like Li_2WO_4 and K_2WO_4 behave quite differently.

The electrical conductivity through the phase diagram is high in the α-phase ($\sigma \sim 10^{-2}$ mho cm^{-1}) almost regardless of composition. The anomalous high conductivity of the β-phase decreases with increasing molybdate content. In pure Na_2MoO_4 an anomaly occurs at the α–α_2 transition, resembling the behavior of Na_2WO_4 at the β–α transition. The (highest) α_2-phase is hexagonal, ($P6_3/mmc$), showing large anisotropic thermal vibrations. The α-phase is orthorhombic (*Fddd*) as is the β-phase (probably $Pbn2_1$).

Introduction

The binary x, T-phase diagram of the Na_2WO_4–Na_2MoO_4 system was measured in 1906 by Boeke (*1*).

Since this was done mainly by cooling curves, and because hysteresis effects of the phase transitions with respect to cooling curves introduce serious errors, we decided to remeasure this phase diagram. To construct the phase diagram, we used DTA heating curves only.

In the further studies, that have been made on these compounds up till recently (*2–6*), there is one important effect that has either been overlooked or has not been paid much attention to. This is the effect of already small amounts (0.1 mole%) of impurities on the phase transitions. In previous work (*7*) we have mentioned the effect of so-called isomorphous dopants on the β–γ transition of Na_2WO_4. In this work we will describe a more systematic study of the effects of SO_4^{2-}, CrO_4^{2-}, Li^+, and K^+ ions on the phase transitions of Na_2WO_4. Furthermore, remeasurements of the transition entropies of Na_2WO_4 and Na_2MoO_4 were performed by using the DSC technique. Previous determinations of these entropies have been done by DTA (*3*) and by drop calorimetry(*8*).

After this thermodynamic study of the phase diagram, we were able to concentrate upon our particular interest in these compounds: Na_2WO_4 has two highly conducting ($\sigma \sim 10^{-2}$ mho cm^{-1}) high-temperature phases. Apart from this high conductivity, it shows an anomaly with respect to its conductivity as a function of temperature: the highest-temperature (α–) phase below the melting point has not the highest conductivity, but rather the second highest (β–) phase, shows the highest conductivity. Until now, no conductivity data were available for either pure Na_2MoO_4 or for Na_2WO_4–Na_2MoO_4 solid mixtures. Thus, we decided to measure the conductivities as a function of temperature for some compositions in the phase diagram, and for pure Na_2MoO_4. A consideration of the structures of the high-temperature phases might pos-

sibly allow for a correlation of the structural properties to the electrical behavior.

Although some structural investigations were made by Pistorius (*6*), the structure elucidation of the high temperature phases was not complete by far. Recent investigations by Van den Berg (*10*) have given more insight into the structural properties and also revealed some other interesting properties of Na_2WO_4. Furthermore, it assisted the interpretation of the phase diagram. Since Van den Berg et al. would not publish their results on Na_2WO_4 and Na_2MoO_4—they have added their results to the A.S.T.M. system—they were so kind to put their results at our disposal, and allowed us to use them in this work.

Experimental

For the experiments "Baker Analyzed" $Na_2WO_4 \cdot 2H_2O$ and $Na_2MoO_4 \cdot 2H_2O$ were used as starting materials.

Previous analysis results had shown that these compounds were sufficiently pure for our purpose: the impurity levels are considerably inferior to our dopant levels.

Both salts were dehydrated at 400°C, atmospheric pressure. By thermogravimetrical analysis (TGA) it was shown that there was no detectable amount of water left in the salts and that no detectable decomposition or sublimation occurred up to 900°C. By weighing adequate amounts of both salts into a porcelain crucible and by heating the crucible for some 5 min at 800°C in an oven, solid mixtures were obtained after cooling to ambient. The crucibles were not at all affected by the molten salt in this short time. The solid mixtures were then ground. In the doping experiments Na_2SO_4, Na_2CrO_4, Li_2WO_4, and K_2WO_4 of chemical pure grade were used. The doped samples were prepared in the same way as the mixtures. Since a check on the homogenity of these doped samples was virtually impossible because of the low concentrations involved, we made large series of measurements. Observation of the scatter in measured quantities then makes an interpretation possible. For the DTA measurements we used a rather simple construction. The sample was placed in an Al_2O_3 crucible (Degussa Al 23) which was fitted into a monel sample holder.

The latter in turn fitted into a small vertical quartz oven, supplied with a programmable temperature controller (Eurotherm, thyristor f.c.). The temperature in the sample was measured with a Pt/Pt-10% Rh couple, placed in the molten sample before each run. The "reference temperature" was measured in the sample holder, directly under the Al_2O_3 crucible. By using an adjustable bias-voltage source and a Knick amplifier, the temperature signal was fed to the horizontal input of an X,Y-recorder, while the amplified difference signal of the measuring and reference couple was fed to the vertical input. After calibration, the absolute accuracy of measured transition temperatures was estimated to be ±2°C.

All measurements were performed in air. In general, heating and cooling rates of 10°C/min were used.

The differential scanning calorimetric measurements were performed by Drs. F. Brants on a Perkin–Elmer DSC-2 commercial apparatus. The samples were contained in gold pans. Quantitative measurement of the transition enthalpies was done by planimetric measurement of the peak surfaces. Calibration was on Zn, as given by the "American Institute of Physics Handbook". For the technique used in the structure determination by Van den Berg et al. we will chiefly confine ourselves to referring to their latest work on a related compound (*9*). X-ray powder diffraction exposures as a function of temperature were made with a Guinier–Lenné camera. The electrical conductivity measurements were made on pressed pellets, which after sintering at 400°C, were supplied with either Ag- or Pt-paint electrodes. The pellets were contained between two specially designed electrodes in a quartz tube oven, also supplied with a thyristor fast cycling temperature controller (Eurotherm). (The electrodes were constructed such as to make Kelvin-type measurements possible. A chromel–alumel thermocouple was contained in the electrode at some 2 mm from the pellet.) The electrical conductivity was measured with a Wayne–Kerr automatic bridge, type B-642, at an angular frequency of $\omega = 10^4$ rad sec^{-1}. Together with the tempera-

ture signal from the chromel–alumel couple, it was followed with a two-channel recorder (Kipp, type BD 9).

Detailed admittance measurements as a function of frequency (in the range $\omega = (10^1 - 2.10^5)$ rad sec^{-1}) have shown (*12*) that in the high-temperature phases at angular frequencies around $\omega = 10^4$ rad sec^{-1} and lower, the frequency dispersion in the admittance behavior is entirely due to interfacial processes. However, the measured G-value at $\omega = 10^4$ rad sec^{-1} corresponds to the extrapolated value (to infinite frequency) for the bulk conductance to within 1 or 2%. Thus, we made no correction for the values, as measured with the automatic bridge.

Results

Phase Diagram

From the DTA measurements as described in the experimental section, heating and cooling curves were obtained. Typical examples are given in Figs. 1 and 2. The transition temperatures were taken at the steepest parts of the curves. Such curves were determined for the Na_2WO_4–Na_2MoO_4 system with intervals of 5 mole% in the middle of the diagram, taking smaller intervals towards the ends. From the transition temperatures of some 50 mixtures, the phase diagram was constructed (Fig. 3). Since the melting temperatures of both salts were almost the same and since the deviation from ideality was apparently small, no solidus–liquidus loop could be measured. It is probably within the experimental scatter. This applies also to the α–β transition, concerning a phase-demixing loop. It will be clear from the next section, that because of the hysteresis effects involved in the phase transitions, one may not use quantitative information from the cooling curves to be used in the phase diagram. Thus, the only information about phase-demixing loops must be obtained from the heating curves. One can, for instance, compare the steepness of the γ–β transitions in the heating curves at different compositions. This should show less steep transitions in the middle of the diagram, because a temperature range should be involved. It proved not to be possible to measure the β–α transition at increasing temperature by means of the DTA technique, when the tunstate mole fraction was more than 0.85, because of the coincidence of the heat effect of this small transition with the large

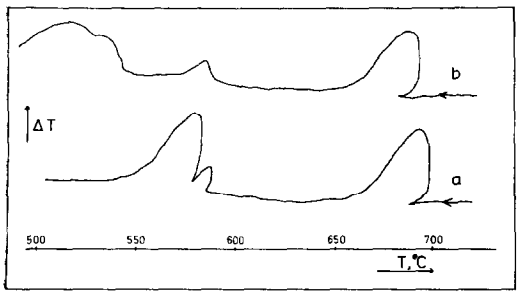

FIG. 1. Typical cooling DTA runs. a. pure Na_2WO_4; b. Na_2WO_4 with 0.49 mole% Na_2WO_4.

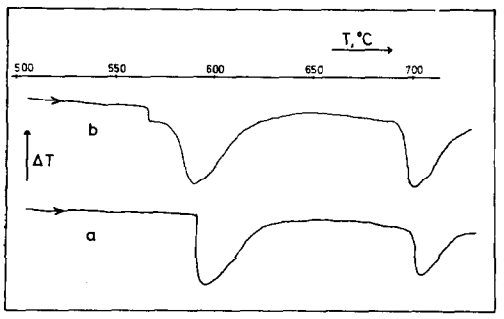

FIG. 2. Typical heating DTA runs. a. Pure Na_2WO_4; b. Na_2WO_4 with 0.53 mole% K_2WO_4.

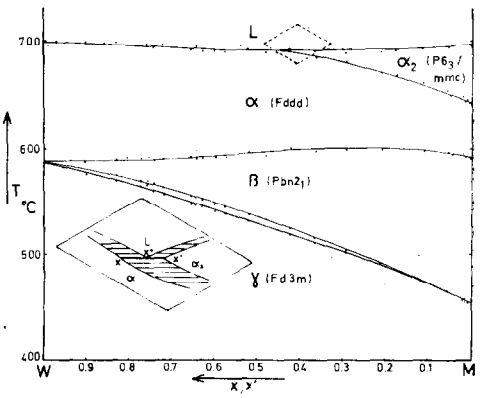

FIG. 3. Phase diagram of the Na_2WO_4–Na_2MoO_4 system; dots are experimental data (from heating DTA runs). W = Na_2WO_4, M = Na_2MoO_4.

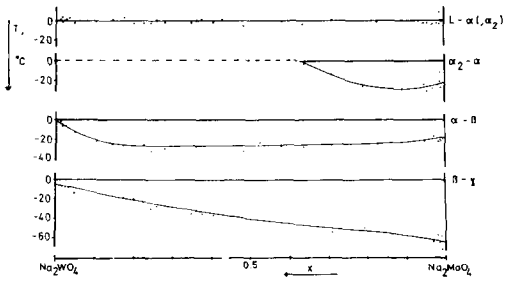

FIG. 4. Hysteresis diagram of the transitions of Na_2WO_4–Na_2MoO_4 mixtures. Data obtained from difference of cooling and heating DTA-runs.

heat effect of the γ–β transition. For pure Na_2WO_4 we were able to separate the transitions by using the DSC technique, at a heating rate of 0.3°C min^{-1}. The real β-range thus measured was 2°C.

A slight "heating-hysteresis" of the γ–β transition may cause the β-range to be measured as only 1°C.

Hysteresis

By comparison of the transition temperatures at heating and cooling DTA curves, the thermal hysteresis of the phase transitions may be obtained. This hysteresis as a function of composition is given in Fig. 4. The large difference in hysteresis for the β–γ transition of Na_2WO_4 and Na_2MoO_4 is remarkable as we will consider further on.

When a cooling rate of 3°C min^{-1} is used for pure Na_2MoO_4, all four transitions split up into a large number of small transitions, while at increasing temperature all transitions behave normal at this rate. Na_2WO_4 showed this effect only for the β–γ transition, and then a ten times lower cooling rate had to be used (0.3°C min^{-1}). This phenomenon was also reported by Hare (*14*). Possibly these effects may be attributed to slow formation of crystallization germs.

Transition Entropies

The DTA plots give already some indication about the magnitude of the heat effects involved in the phase transitions. However, a quantitative interpretation of DTA is erroneous in many cases and very "tricky" in all cases. Denielou et al. used drop calorimetry to determine the transition enthalpies (*8*). However, they did not mention two transitions for Na_2WO_4 but only one, obviously because the small β-range made a separation impossible. With DSC it proved to be possible to measure all separate transitions quantitatively, after calibration on Zn.

The results of our measurements, together with the literature data, are given in Table I.

TABLE I

MOLAR TRANSITION ENTROPIES OF Na_2WO_4 AND Na_2MoO_4. TRANSITION ENTROPIES ARE GIVEN IN EMU (cal K^{-1})

	Na_2MoO_4		Na_2WO_4		
Transition	Denielou et al. (*8*)	This work	Goranson–Kracek (*3*)	Denielou et al. (*8*)	This work
L–α	5.32 ± 0.12	5.12 ± 0.10	5.95 ± 0.30	6.89 ± 0.14	7.51 ± 0.15
L–α_2	(T = 962 K)	(T = 963 K)	(T = 969 K)	(T = 967 K)	(T = 967 K)
α_2–α	2.16 ± 0.12	2.01 ± 0.08			
	(T = 915 K)	(T = 913 K)			
α–β	0.58 ± 0.10	0.52 ± 0.05	1.16 ± 0.06		1.20 ± 0.02
	(T = 866 K)	(T = 865 K)	(T = 862 K)		(T = 863 K)
				8.77 ± 0.14	
β–γ	7.24 ± 0.13	7.89 ± 0.16	8.68 ± 0.43	(T = 859 K)	7.76 ± 0.16
	(T = 718 K)	(T = 734 K)	(T = 861 K)		(T = 861 K)

The results are in good agreement. The summed heat effect by Denielou for the "γ–α transition" of Na_2WO_4 equals the sum of the γ–β and β–α transitions as we measured them.

Dopant Effects

Because of the observed influence of very small amounts of impurities on the β–γ transition of Na_2WO_4 (*7*), the effects were investigated more extensively, using two "anion" and two "cation" dopes.

Anion Dopes

As anion dopes, SO_4^{2-} and CrO_4^{2-} were chosen. These ions showed to have only a slight influence upon the temperature of the γ–β transition at increasing temperature and upon the temperature of the α–β transition in both directions. Possible systematic changes are largely obscured by the observed scatter. The β–γ transition, however, showed to have a clear large thermal hysteresis, caused by these anion dopes (Fig. 5). A typical example of a cooling DTA-run with 0.49 mole% SO_4^{2-} is shown in Fig. 1b. The transition seems to be "smeared out" over a certain temperature range. If the sulfate content is taken higher than 1 or 2 mole%, then this effect makes it almost impossible to assign a transition temperature. These effects are reflected in electrical conductivity measurements; at high dopant contents it may take days for the phase transition to be completed. The results of the dopant measurements were plotted in the form log[dopant] vs T just for convenience. Whether an empirical linear relation of this form would hold more generally is speculative, since very few literature data of this kind are available. (A theoretical explanation of the dopant effect may not yet be given.)

The much larger scatter in the results for sulfate than for chromate may have to do with the closer relationship of chromate to tungstate, the mean effects of both dopants, however, are almost the same.

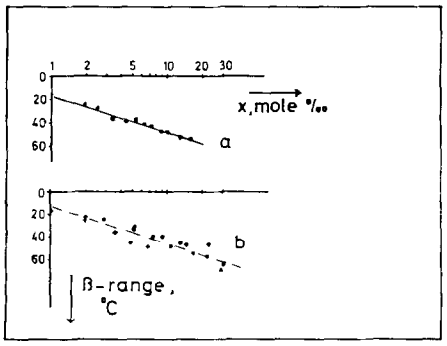

FIG. 5. Metastable extension of β-phase of Na_2WO_4, caused by introducing anion dopes (mole‰ = 10 × mole%). a. CrO_4^{2-} dope; b. SO_4^{2-} dope.

Cation Dopes

Li^+ and K^+ were chosen as cation dopes for Na_2WO_4. Quite different from the anion dopes, Li^+ only slightly affects the β–γ transition in the cooling curves; the thermal hysteresis of this transition does not exceed some 20°C with dopant concentrations up to 0.03 mole fraction of Li_2WO_4. However, Li^+ does affect the α–β transition quite markedly; the α–β transition temperature is increased with increasing Li^+ content. Also in the Li^+ doped samples, there is no thermal hysteresis of the α–β transition. K^+ has virtually no effect on the magnitude of the β-range at concentrations lower than 0.03 mole fraction. Both the $L \rightarrow \alpha$, $\alpha \rightarrow \beta$ and $\beta \rightarrow \gamma$ transitions are lowered in temperature with already low K^+ content (giving a decrease of some 10°C when $[K^+]$ is 0.005 mole fraction). A quite remarkable new transition comes up in the heating curves with K^+ contents as low as already 0.002 mole fraction, at a temperature of 565°C. In Fig. 2b we have given an example of such a heating run. With DSC it was confirmed that a new transition is indeed involved, since the $\gamma \rightarrow \beta$ and $\beta \rightarrow \alpha$ transitions may still be found at low heating rate, and since their proportional heat effects remain unchanged in the doped samples. We have strong evidence that K_2WO_4 is segregated completely from Na_2WO_4 at ambient within a few months, since the new transition in the heating curves is only seen with "freshly" prepared samples. Older samples (2–3 mo) must be remolten first, before showing the effect.

Electrical Conductivity

The results of the electrical conductivity measurements on samples containing 17.2 and

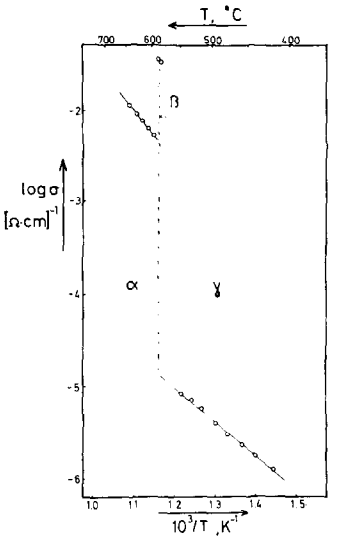

FIG. 6

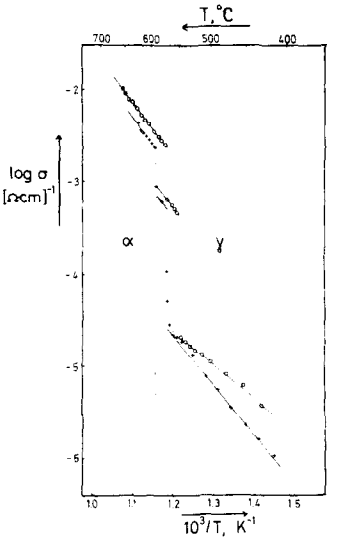

FIG. 7

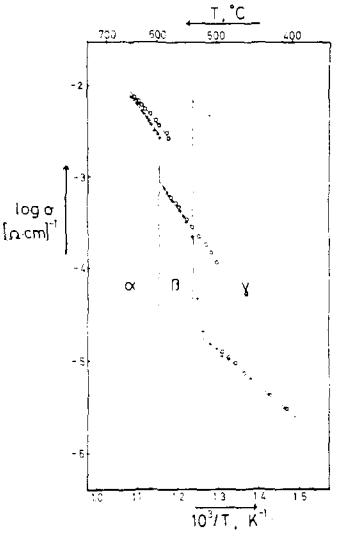

FIG. 8

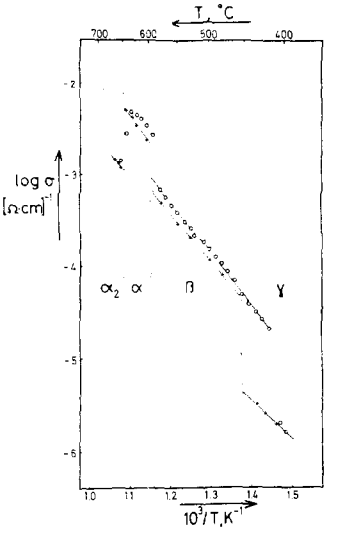

FIG. 9

FIGS. 6–9. Electrical conductivities of Na_2WO_4, Na_2MoO_4, and two mixtures; $\log\sigma$ vs $1/T$ plots. Fig. 6. Na_2WO_4; Fig. 7. Na_2WO_4 (82.8%) + Na_2MoO_4; Fig. 8. Na_2WO_4 (51.9%) + Na_2MoO_4; Fig. 9. Na_2MoO_4.

48.1 mole% of Na_2MoO_4 and on the pure compounds are plotted in the form $\log\sigma$ vs T^{-1} (Figs. 6–9). First of all, it is noticed that the anomalous behavior of the β-phase, as mentioned in the introduction, does not occur in the case of 17.2 mole% molybdate, neither at higher molybdate contents.

In pure Na_2MoO_4 the remarkable fact is, that it is now the α-phase which conducts better than the α_2-phase. For convenience we have summarized the results of the conductivity measurements in Table II. For the α-phase there seems to be a tendency for the preexponential factor to increase somewhat with increasing tungstate content. This effect is even more marked for the β-phase. Notice, that in Fig. 7 the isothermal points for the γ-phase at increasing temperature give a larger slope than at decreasing temperature. This is the only represented case where we have

TABLE II

CONDUCTIVITY PARAMETERS IN THE Na_2WO_4–Na_2MoO_4–SYSTEM[a]

Composition[c]	γ-phase		Δ[b]	β-phase		Δ[b]	α-phase		Δ[b]	α_2-phase		
	σ_o	ε	$\gamma \rightarrow \beta$	σ_o	ε	$\beta \rightarrow \alpha$	σ_o	ε	α–α_2	σ	ε
1	$\sim 10^{-4}$	0.71	+3.4	2×10^{-1}	~1.1	−0.8	3.6×10^{-2}	1.10			
2	$\sim 10^{-4}$	0.75	+1.3	7.5×10^{-3}	1.16	+0.5	3.0×10^{-2}	1.12			
3	$\sim 10^{-4}$	0.75	+1.1	7.5×10^{-3}	1.18	+0.5	2.6×10^{-2}	1.23			
4	$\sim 10^{-4}$	0.75	+1.0	7.0×10^{-3}	1.12	+0.5	1.8×10^{-2}	1.18	−0.7	3.4×10^{-3}	1.18

[a] Given in the form: $\sigma(T) = \sigma_o \exp(-\varepsilon/kT)$. ($\sigma_o$ in mho cm^{-1}, ε in eV).

[b] Δ is the jump in decades of log σ at the transition temperature. Notice that a negative Δ-sign represents an anomalous case.

[c] Compositions: 1. pure Na_2WO_4; 2. 82.8 mole% Na_2WO_4; 3. 51.9 mole% Na_2WO_4; 4. pure Na_2MoO_4.

measured at increasing temperature before measuring at decreasing temperature. The origination of the different slopes for the γ-phase probably involves a number of effects, i.e., sintering and surface conduction. Since we are mainly interested in the highly conducting phases, we will not go into more detail about this. With increasing temperature it is generally seen that the conductivity in the γ-phase in the vicinity of the γ–β transition is somewhat higher than would be expected. This effect is most marked in the 50% case (Fig. 8), which may well be due to the temperature range involved in the phase demixing loop. By comparison of the isothermals at decreasing and those at increasing temperature one finds, that here too thermal hysteresis occurs. The conductivities are measured isothermally over at least several hours and in many cases over a day. Still the hysteresis involved in each phase transition as found from the conductivity measurements and those from the DTA measurements (Fig. 4) are almost equal. So it seems that these hysteresis effects are little dependent upon the cooling rate. The mentioned "breaking up" of phase transitions at low cooling rate was, however, not reflected in the conductivity measurements.

Structural

Van den Berg et al. (*10*) made powder diffraction exposures for both pure Na_2WO_4 and Na_2MoO_4 and for mixed crystals, in the temperature range 400–670°C, thus covering all the solid phases.

First of all, the powder diffraction results underline the conclusion drawn from the phase diagram, namely the complete intersolubility of both salts. Furthermore, the α- and β-phases seem to be closely related, both in symmetry and in cell dimensions. Though at ambient temperature the cell dimension of the γ-phase (cubic spinel) of Na_2WO_4 and Na_2MoO_4 show a slight difference (Table III), the cell dimensions are almost independent of composition in the phase diagram at the temperature of the γ–β transition (in Fig. 3 along the line separating the γ and β-phase).

Both pure Na_2WO_4 and Na_2WO_4-rich mixtures show a strong tendency for single crystal growth or preferential orientation in the α- and β-phases. This makes an interpretation of the powder data very difficult. Essentially, however, this could imply the possibility of performing single crystal measurements, for instance with the technique used previously by Van den Berg (*9*).

A complete structure determination was not possible for β-Na_2MoO_4 from the powder data. Single crystal measurements on the β-phase of the tungstate as suggested, could help in this aspect. The results of the structure determinations are given in Table III.

Discussion

Thermodynamical analysis of experimental data—covering both the shape of the phase diagram and the measured values of transition entropies—can give some insight into the

TABLE III

STRUCTURES OF VARIOUS PHASES IN THE PHASE DIAGRAM Na_2WO_4–Na_2MoO_4

α_2-phase	Hexagonal, space group $P6_3/mmc$				
	For pure Na_2MoO_4 the cell parameters at $T = 664$°C are:				
(*10*)	$a = b = 5.934$ Å, $c = 7.549$ Å, $Z = 2$. $V/Z = 115.0$ (Å)^3.				
	(Contribution of $\frac{1}{2}$- and $\frac{1}{4}$ atoms represent disorder situation)				
			x	*y*	*z*	*contribution*
	Atomic positions	Mo	1/3	2/3	0.742	$\frac{1}{2}$ atom
		Na_1	0	0	0.033	$\frac{1}{2}$ atom
		Na_2	1/3	2/3	0.192	$\frac{1}{2}$ atom
		O_1	1/3	2/3	0.968	$\frac{1}{2}$ atom
		O_2	0.192	0.838	0.667	$\frac{1}{4}$ atom
α-phase	Orthorhombic, space group *Fddd*				
	For pure Na_2MoO_4 the cell parameters at $T = 613$°C are:				
(*10*)	$a = 12.88$ Å, $b = 10.19$ Å, $c = 6.48$ Å, $Z = 8$. $V/Z = 113.9$ (Å)^3				
			x	*y*	*z*	
	Atomic positions	Mo	0	0	0	
		Na	0	0.315	0	
		O	0.0750	0.0885	0.149	
β-phase	Orthorhombic, space group most probably $Pbn2_1$.					
	For pure Na_2MoO_4 the cell parameters at $T = 563$°C are:					
(*10*)	$a = 10.88$ Å, $b = 7.17$ Å, $c = 17.33$ Å, $Z = 12$. $V/Z = 112.7$ (Å)^3.					
	(Precise structure determination impossible from powder data)					
γ-phase	Cubic, space group $Fd3m$ Spinel					
(*11*)	Na_2MoO_4 (25°C): $a = 9.108$ Å, $Z = 8$. $V/Z = 94.4$ (Å)^3					
	Na_2WO_4 (25°C): $a = 9.130$ Å, $Z = 8$. $V/Z = 95.1$ (Å)^3.					

interactions involved in this system. An extensive treatment of the thermodynamical aspects is presently beyond our scope, but we can mention some results. First of all it can be verified, whether the composition, at the temperature, where the α_2–α and liquid phases are in equilibrium, is correct. Thermodynamically there must be three compositions involved, according to the phase-demixing into the three phases. If this calculation is performed on basis of ideal intersolution behavior, one finds that $x(\alpha) = 0.468$, $x'(\alpha_2) = 0.443$, $x''(L) = 0.450$.

Such precise data may not be obtained from the phase diagram, as obviously the differences between x, c', and x'' are within the experimental scatter. The mean value, however, agrees well with the phase diagram. Another feature involves the calculation of an excess enthalpy parameter for the β-phase. It is then assumed that the higher-temperature phases behave ideally, and that the β-phase behaves parabolically regular, i.e., $\Delta H_\beta^E = b_\beta x(1 - x)$. The molar excess enthalpy parameter thus found is, $b_\beta = -27 \pm 3$ cal. This interaction difference is so small as compared with the RT-level ($RT \sim 1800$ cal), that one may safely consider the β-, α-, α_2, and L-phases as exhibiting ideal behavior. The shape of the phase-demixing loop for the β–γ transition points to nonideal thermodynamic behavior in the γ-phase. The effect of sulfate and chromate dopants on the β–γ transition at decreasing temperature is not yet fully under-

stood. Apart from the decrease of the transition temperature, one finds that the sluggishness of the transition is enforced. This is reflected in the "smearing out" of the transition over a large temperature range (Fig. 1b). The effect of potassium and lithium ions may possibly be explained by further investigations of the Na_2WO_4–Li_2WO_4 and the Na_2WO_4–K_2WO_4 phase diagrams. As dopants these ions seem to be of little interest. It seems somewhat remarkable that the hysteresis effects exhibited by the phase transitions in pure Na_2MoO_4 are so much larger than those for pure Na_2WO_4. Rao and Rao (*13*) pointed out that there is a correlation between the thermal hysteresis and the volume changes at the phase transitions. We checked our results for such a correlation. From the work of Pistorius, we took the slopes dp/dT for any one of the phase transitions and by using the Clapeyron equation and our entropy data, the volume changes at the phase transitions were calculated. They are summarized in Table IV, together with the average hysteresis effects found. There appears to be no correlation.

It seems that a number of properties with respect to the interaction of molybdate and tungstate lattices and with respect to the electrical behavior should be carefully discussed by correlation to precise structure data. However, there are still some problems in this respect. A precise structure determination, involving the determination of lattice parameters as a function of temperature, is only possible by using an internal standard, which should be inert with respect to the material to be investigated. α-Al_2O_3, which is commonly used, proved to be impracticable. Furthermore, tungstate-rich mixtures cannot be investigated by powder methods in their high-temperature phases. Single crystal measurements would enable the determination of precise data; however, they are difficult to perform.

On basis of transport number determinations still in progress we have sufficient evidence that in all of the solid phases, Na^+ migration is the major contribution to the conduction process.

It is presently rather well known that at ambient temperature Na_2WO_4 and Na_2MoO_4 have the spinel arrangement. In such an arrangement one may expect the cationic mobility to be low, which is reflected in the electrical conductivity of the γ-phase. Since a precise structure determination was not yet

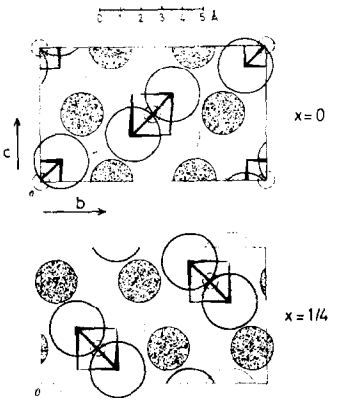

FIG. 10. Structure of α-phase in the Na_2WO_4–Na_2MoO_4 system. α-phase is D_{4h}^{24}-(*Fddd*) (*10*). Large circles represent oxygen, smaller circles, sodium ions.

TABLE IV

VOLUME CHANGES AND THERMAL HYSTERESIS EFFECTS AT THE PHASE TRANSITIONS IN PURE Na_2WO_4 AND PURE Na_2MoO_4

Transition	ΔV cm^3/g	ΔV $(Å)^3$/molecule	Thermal hysteresis °C
α–β Na_2WO_4	0.000	0.000	1
β–γ Na_2WO_4	0.038	0.16	5
α_2–α Na_2MoO_4	−0.002	−0.008	20
α–β Na_2MoO_4	−0.0005	−0.002	15
β–γ Na_2MoO_4	0.045	0.15	65

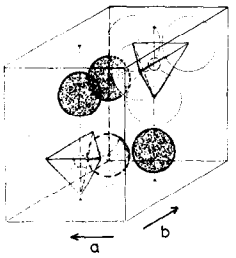

FIG. 11. Structure of α_2-phase in the Na_2WO_4–Na_2MoO_4 systems. α_2-phase is $P6_3/mmc$. Large circles represent oxygen, smaller circles sodium ions.

possible for the β-phase, we will not take this phase into consideration here. For the α-phase, the structure is rather "open" (Fig. 10). In all three directions there is enough room for the sodium ions to migrate. Possibly cooperative cation migration is involved. In the α_2-phase there is a large disorder in both the cationic and anionic sublattices (Fig. 11). This may either be interpreted in terms of large anisotropic thermal vibrations or in terms of Frenkel orientation disorder. It is well possible, that in the α_2-phase the disorder in the anionic sublattice interferes with the cationic migration, resulting in decreased conductivity with respect to the α-phase (for instance by scattering processes).

Conclusions

It has become clear in this work, that in the construction of a phase diagram, one should be cautious in using cooling DTA runs, because of the thermal hysteresis effects involved in certain phase transitions. Very low concentrations of related compounds may also have a very marked influence. One should keep this in mind when using certain compounds as temperature standards: The "standard" temperature might be very sensitive to the purity of the compound (for instance chromates are presently sometimes used as temperature standards).

As for the electrical conductivity, it is quite clear that the "room" available in a certain structure for the cationic migration, gives a reasonable indication about the possible high conductivity of that "phase." The magnitude of the transition entropies may point in the same direction: if there is a large entropy of transition, then one may expect a large jump in the electrical conductivity.

Acknowledgments

We would like to express our gratitude to Ir. A. J. van den Berg and Dr. F. Tuinstra of the Technical Physics Laboratory of the Technische Hogeschool Delft, for the nice cooperation on this subject and for allowing us to publish their structural results. We would also like to thank Drs. F. Brants of the Crystal Chemistry Department of the State University Utrecht for performing the DSC measurements and for his help in their interpretation. We would like to thank Dr. G. H. J. Broers for many profitable discussions, for stimulating the cooperation with the people from Delft, and for his careful reading of the manuscript. Mr. F. Broersma is acknowledged for performing the TGA measurements.

References

1. H. E. BOEKE, *Z. Anorg. Chem.* **50**, 355 (1906).
2. H. S. VAN KLOOSTER AND H. C. GERMS, *Z. Anorg. Chem.* **86**, 369 (1914).
3. R. W. GORANSON AND F. C. KRACEK, *J. Chem. Phys.* **3**, 87 (1935).
4. G. H. J. BROERS, Ph.D. thesis, Amsterdam (1958).
5. F. HOERMANN, *Z. Anorg. Chem.* **177**, 145 (1929).
6. C. W. F. T. PISTORIUS, *J. Chem. Phys.* **44**, 4532 (1966).
7. P. H. BOTTELBERGHS *in* "Fast Ion Transport in Solids" (W. van Gool, Ed.), p. 637. North-Holland, Amsterdam, 1973.
8. L. DENIELOU, Y. FOURNIER, J. P. PETITET, AND C. TEQUI, *C.R. Acad. Sci. Paris* **t272**, C1855 (1971).
9. A. J. VAN DEN BERG, F. TUINSTRA, AND J. WARCZEWSKI, *Acta Cryst.* **B29**, 586 (1973).
10. A. J. VAN DEN BERG, AND F. TUINSTRA, private communication.
11. H. SWANSON, M. MORRIS, R. STINCHFIELD, AND E. EVANS, *N.B.S.* monograph **25**, 47 (1962).
12. P. H. BOTTELBERGHS, to be published.
13. K. J. RAO AND C. N. R. RAO, *J. Mat. Sci.* **1**, 238 (1966).
14. A. HARE, *Phil, Mag.* **48**, 418 (1924).